


Simulation and optimization framework for evaluating the robustness of low-impact development placement solutions under climate change in a small urban catchment

César Ambrogi Ferreira do Lago, Abtin Shahrokh Hamedani, Eduardo Mário Mendiondo & Marcio Hofheinz Giacomoni


To cite this article: César Ambrogi Ferreira do Lago, Abtin Shahrokh Hamedani, Eduardo Mário Mendiondo & Marcio Hofheinz Giacomoni (2023) Simulation and optimization framework for evaluating the robustness of low-impact development placement solutions under climate change in a small urban catchment, *Hydrological Sciences Journal*, 68:14, 2057-2074, DOI: [10.1080/02626667.2023.2248137](https://doi.org/10.1080/02626667.2023.2248137)

To link to this article: <https://doi.org/10.1080/02626667.2023.2248137>

 View supplementary material [↗](#)

 Published online: 02 Nov 2023.

 Submit your article to this journal [↗](#)

 Article views: 101

 View related articles [↗](#)

 View Crossmark data [↗](#)

Simulation and optimization framework for evaluating the robustness of low-impact development placement solutions under climate change in a small urban catchment

César Ambrogi Ferreira do Lago^a, Abtin Shahrokh Hamedani^a, Eduardo Mário Mendiondo^b and Marcio Hofheinz Giacomoni^a

^aSchool of Civil & Environmental Engineering, and Construction Management, The University of Texas at San Antonio, San Antonio, Texas, USA; ^bSao Carlos School of Engineering, University of Sao Paulo, São Carlos, Brazil

ABSTRACT

The lack of acceptable temporal resolution of climate projections hinders proper assessment of the future performance of low-impact development (LID) systems in small catchments when continuous simulations are required (e.g. to evaluate infiltration). This study applied a simulation optimization approach to maximize infiltration with LIDs at minimum costs in a small urban catchment (0.67 km²). We coupled the Storm Water Management Model (SWMM) with the Nondominated Sorting Genetic Algorithm II (NSGA-II) to determine near-optimal locations of bioretentions, green roofs, and permeable pavements. The temporal resolution of rainfall projections was disaggregated from 24 hours to 15 minutes using the Bartlett-Lewis rectangular method to evaluate the performance and robustness of the optimized solutions under different budgets and climate scenarios. Results suggest that LIDs can mitigate climate change impacts with relatively inexpensive solutions. However, the robustness analysis showed that climate change could compromise the expected performance of LIDs sized with historical rainfall.

ARTICLE HISTORY

Received 29 June 2022
Accepted 7 July 2023

EDITOR

S. Archfield

ASSOCIATE EDITOR

S. Ochoa Rodriguez

KEYWORDS

climate change; low-impact developments; multi-objective optimization; robustness; NSGA-II

1 Introduction

Climate change is likely to magnify the frequency and severity of droughts (Nam *et al.* 2015, Heinemann *et al.* 2017, Marcos-Garcia *et al.* 2017, Ahmed *et al.* 2018, Ayanlade *et al.* 2018, Wang *et al.* 2018), while increasing the frequency and intensity of extreme rainfall (Aich *et al.* 2016, Shrestha *et al.* 2016, Clavet-Gaumont *et al.* 2017, Yin *et al.* 2018, Gao *et al.* 2020). As a consequence of a drier future climate, aquifer recharge capacity can be reduced (Shrestha *et al.* 2016), thus impacting water availability, particularly in regions where aquifers are the primary source of freshwater supply. On the other hand, flood events can become more frequent and hazardous (Sun *et al.* 2016, 2017, do Lago *et al.* 2021). Low-impact development (LID) uses stormwater control measures (SCMs) to reestablish the pre-development hydrological conditions by increasing infiltration, reducing pollutants in the source (Fletcher *et al.* 2013), and restoring ecosystem services (Batalini de Macedo *et al.* 2022). Furthermore, LID can alleviate the impacts of climate change (Charlesworth 2010, Fletcher *et al.* 2013, de Macedo *et al.* 2021). LID can help restore aquifer recharge by promoting infiltration, especially in a drier climate when the water table is low, and a higher fraction of infiltrated volume can be converted into recharge (Mooers *et al.* 2018).

The ability of LID to alleviate the impacts of urbanization and climate change depends on suitable design and placement (Refsgaard *et al.* 2013), as well as proper long-term maintenance (Brown and Hunt 2012, de Macedo *et al.* 2017). Furthermore, upstream land use modifications and climate

change can also affect the efficiency of LID practices (Carolus *et al.* 2020, Batalini de Macedo *et al.* 2022), evidencing the necessity to estimate LID's future performance under different scenarios. Assessing the most cost-effective combination of LID controls in an urban watershed is challenging due to the size of the decision space: multiple possible locations, types of SCMs, and design characteristics (e.g. areas, volumes, materials, etc.). In addition, the multiple LID benefits also add complexity to decision making, as different placements and types of SCMs contribute differently to achieving specific hydrological objectives. For instance, the most cost-effective LID configurations designed to reduce runoff volume are likely not the same as those when the goal is to improve stormwater quality or enhance ecosystem services.

Simulation models and optimization algorithms can be used to identify the number, location, and types of LID systems to be installed in a watershed (Helmi *et al.* 2019). Studies in the literature have used simulation and optimization algorithms to optimize LID implementation. Most studies seek to minimize peak flows, runoff volumes, and pollutant loads (Baek *et al.* 2015, Eckart *et al.* 2018, Huang *et al.* 2018, Helmi *et al.* 2019, Tansar *et al.* 2022). The Non-dominated Sorting Genetic Algorithm II (NSGAI) is one common algorithm used to optimize LID placement. For instance, Giacomoni and Joseph (2017) evaluated the tradeoff between cost and hydrological metrics such as peak flow, runoff volume, and hydrological footprint residence (HFR) with the use of NSGA-II, where the HFR metric is the integral of the flooded area over the event time (Giacomoni *et al.* 2012). Kumar *et al.* (2022)

coupled the Storm Water Management Model (SWMM) with NSGA-II to find the optimum number of LIDs for flood control. Azari and Tabesh (2022) maximized the sustainability index of LIDs (which included reliability, resiliency, and vulnerability indices) by coupling NSGA-II with SWMM. Most optimization studies focused on reducing peak flows and runoff volumes (Taghizadeh *et al.* 2021), with a few focusing on improving water quality (Baek *et al.* 2015, Taghizadeh *et al.* 2021). Despite the abundance of studies optimizing LIDs, the surveyed literature indicates a lack of investigations looking to optimize infiltration, which is one of the major objectives of many LID-SCMs.

Although optimized LID systems have been shown to be effective in improving water quality and restoring aspects of the pre-development flow regime, their robustness is less understood due to the uncertainties of climate change (Wang *et al.* 2020). The literature on climate change has proposed methods for managing future climate uncertainties through a multi-model probabilistic approach, which incorporates different scenarios based on various climate projections (Kundzewicz *et al.* 2018). For instance, Liu *et al.* (2017) used rainfall projections from 17 general climate models (GCMs) to optimize the cost–benefit ratio of LIDs in an urban catchment. Moreover, robustness metrics could be used to address these uncertainties by evaluating the performance of water infrastructures under different scenarios. A robust structure performs satisfactorily under various sets of plausible conditions other than what it was designed for (Herman *et al.* 2015, McPhail *et al.* 2018). For instance, Kasprzyk *et al.* (2013) used the robustness metrics to optimize a water supply system, using a simulation and optimization approach to identify plausible solutions with a high level of performance under different future conditions and to facilitate the decision making process. Ng *et al.* (2020) optimized a drainage system using multiple possible design storms to minimize floods and costs through pipe expansion and the use of LID-SCMs. Giese *et al.* (2019) evaluated the robustness of green infrastructure at a watershed scale and concluded that the green infrastructure could help mitigate the increased runoff induced by climate change by enhancing groundwater infiltration and evapotranspiration. These examples show how robustness can support decision makers when uncertainties is significant.

In the available literature, most studies use design storms for evaluating the robustness of LIDs under climate change for different return periods (Yu *et al.* 2022); however, design storms are unsuitable for modeling and optimization of infiltration. Furthermore, literature is still scarce on detailed methods for evaluating LIDs with continuous simulation, especially for micro-drainage where high temporal resolution of rainfall data is required. Micro-drainage refers to a localized, small-scale stormwater management approach that focuses on controlling and treating runoff from precipitation events at or near its source. Although it is possible to obtain three-hour rainfall data from regional climate models (RCMs) (Sim *et al.* 2018), a shorter temporal resolution may still be required. For instance, Berne *et al.* (2004) recommend a temporal resolution of five minutes for catchments on the order of 1000 ha and a three-minute resolution for catchments on the order of 100 ha.

Our investigation showed that the existing literature lacks methods to optimize and evaluate solutions under climate uncertainties concerning infiltration. Therefore, this article applies a simulation-optimization framework to investigate the capabilities of LID placement solutions to mitigate climate change impacts on infiltration, in particular. This study implemented a multi-objective optimization to enhance the cost–benefit ratio of LIDs to increase infiltration in an urban watershed in San Antonio, Texas, located on top of the Edwards Aquifer recharge zone. Climate change projections suggest groundwater recharge is likely to decrease in Texas (Yoon *et al.* 2018), and LID implementation can help to mitigate climate change’s adverse impacts by enhancing infiltration.

A multi-objective optimization to minimize cost and peak flow was also performed for comparative analysis of the typical objectives found in the literature. The robustness of the optimized solutions was evaluated against different future climate scenarios using 25 years of continuous simulation. The projected rainfall patterns were bias-corrected and disaggregated to be suitable for a small-scale catchment. This article presents the following novel contributions to the field of LID and stormwater management: (1) a detailed description of a modeling framework for evaluating mitigating effects of LIDs under climate change with continuous simulation in a catchment with a short time of concentration; (2) an investigation of tradeoffs between infiltration, flood control, and implementation costs; and (3) incorporated climate uncertainty and robustness to evaluate the optimized cost-infiltration and cost-peak solutions.

This paper is divided into three main sections: Methodology, Results and discussion, and Summary and conclusions. In the Methodology section, we describe the hydrological model used in our study and how we processed the climate data as inputs. Next, we explain how we coupled the hydrological model with an optimization algorithm to find cost-effective solutions for placing LIDs. The final subsection of the Methodology describes how we evaluated the solutions to address the challenge of climate uncertainty. In the Results and discussion section, we analyze the LID solutions for different budgets and demonstrate how the type and location of LIDs contribute to achieving various hydrological goals, such as improving infiltration or reducing peak flow. We then evaluate the performance and resilience of the solutions under different climate scenarios. Finally, the Summary and conclusions section presents the paper’s main findings and highlights our methods’ limitations. We also discuss future directions and research opportunities.

2 Methodology

The overall methodology is suitable for application in any catchment, and consists of (1) collecting and treating climate data, (2) optimizing the location of LIDs, and (3) evaluating the optimized solutions (Fig. 1).

First, bias correction of rainfall projected by climate models should be performed. Then, the historical observed rainfall data is used to calibrate and validate the parameters of the bias correction. Due to a large number of climate models,

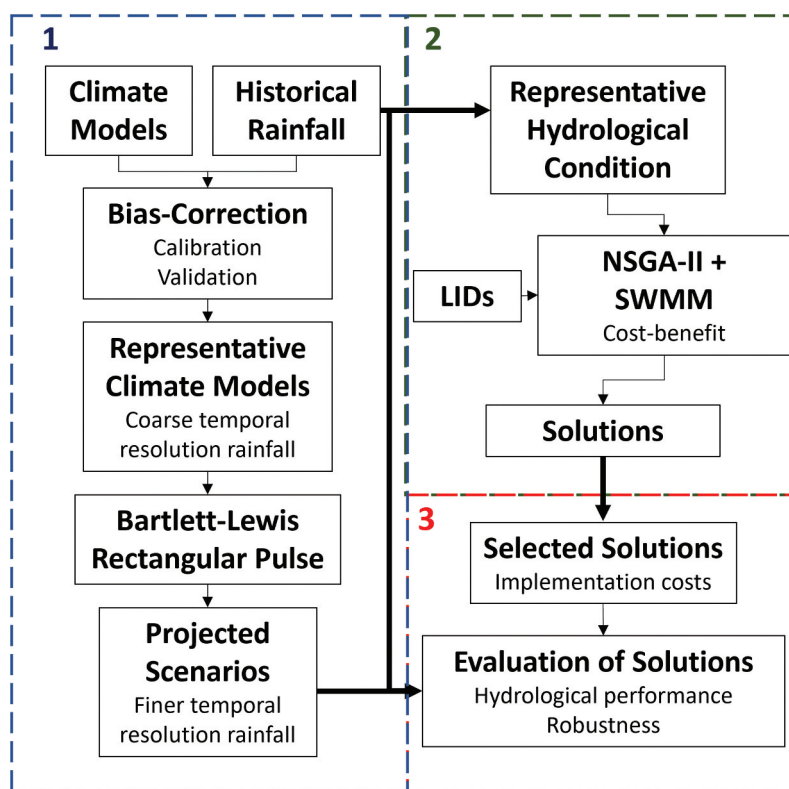


Figure 1. Methodology flowchart. The three main steps are (1) treating climate data, (2) optimizing LID placement, and (3) evaluating the solutions.

representative projections were selected based on the validation of the bias-corrected models. The outputs of climate models usually present a coarser temporal resolution, which is unsuitable for simulating smaller catchments with a short time of concentration. Therefore, the representative was disaggregated into rainfall series with finer temporal resolution using the Bartlett-Lewis rectangular pulse method (Rodríguez-Iturbe *et al.* 1987, Rodríguez-Iturbe *et al.* 1988). This disaggregation was also applied to the historical period to avoid biases when comparing the current and future conditions.

Second, we used the NSGA-II algorithm connected to SWMM to optimize the cost-benefit ratio of LID placement. We optimized the hydrological benefits of LIDs in improving infiltration at a minimum cost (IC). We also minimized peak flow and costs (PC) for comparison purposes, which is a common multi-objective used for LID placement problems. To reduce the optimization time, only one representative year and event from the disaggregated historical series were used for IC and PC, respectively.

Finally, we selected optimized solutions based on implementation costs to estimate their performance under different climate scenarios. The solutions were evaluated based on the hydrological benefits of investing in LIDs and their robustness against different climate scenarios.

2.1 Study area and hydrological modeling

We exemplify the application of the above methodology in the main campus of the University of Texas at San Antonio (UTSA), located on top of the Edwards Aquifer's Recharge Zone (EARZ), which is the primary source of drinking water

within the region. The watershed is 0.67 km² with an average slope of 5%. The area is 62.5% impervious, including approximately 80 institutional buildings and housing three athletic fields and eight parking lots. The studied area is classified under Köppen-Geiger climate Cfa, with a historical average precipitation of approximately 780 mm and a mean annual temperature of 21°C (Peel *et al.* 2007, Zarezadeh 2017).

The Environmental Protection Agency (EPA) SWMM (Rossman and Bernagros 2019) version 5.1014 was used to simulate the UTSA main campus watershed (Zarezadeh 2017), which was sub-divided into 163 sub-catchments. SWMM was used as it is one of the most popular and trustable hydrological models applied to evaluate LID practices (Zhang *et al.* 2014). The SWMM model was built using a 1 m resolution digital elevation model created with data from a light detection and ranging (LiDAR) survey (TNRIS 2020). The campus sewer system is separated, and the drainage network was modeled in SWMM with 3805 m drainage conduits with 93 junctions composed of circular sewers, rectangular sewers, and irregular open-channel swales (Fig. 2). The irregular channel section includes a bioswale of approximately 200 m in the upstream portion, while the remainder is a natural segment. The irregular section also contains two culverts not modeled with SWMM. The model also incorporates one sand filter basin with no seepage loss due to an impermeable liner, which is a regulatory requirement. The sand filter basin's location and drainage area are shown in Fig. 2. The curve number (CN) model (Cronshey 1986) was used to estimate infiltration, with an average CN of 89, and the kinematic wave method was used to route surface runoff using a 15-second time step. The evaporation rate was calculated using minimum and

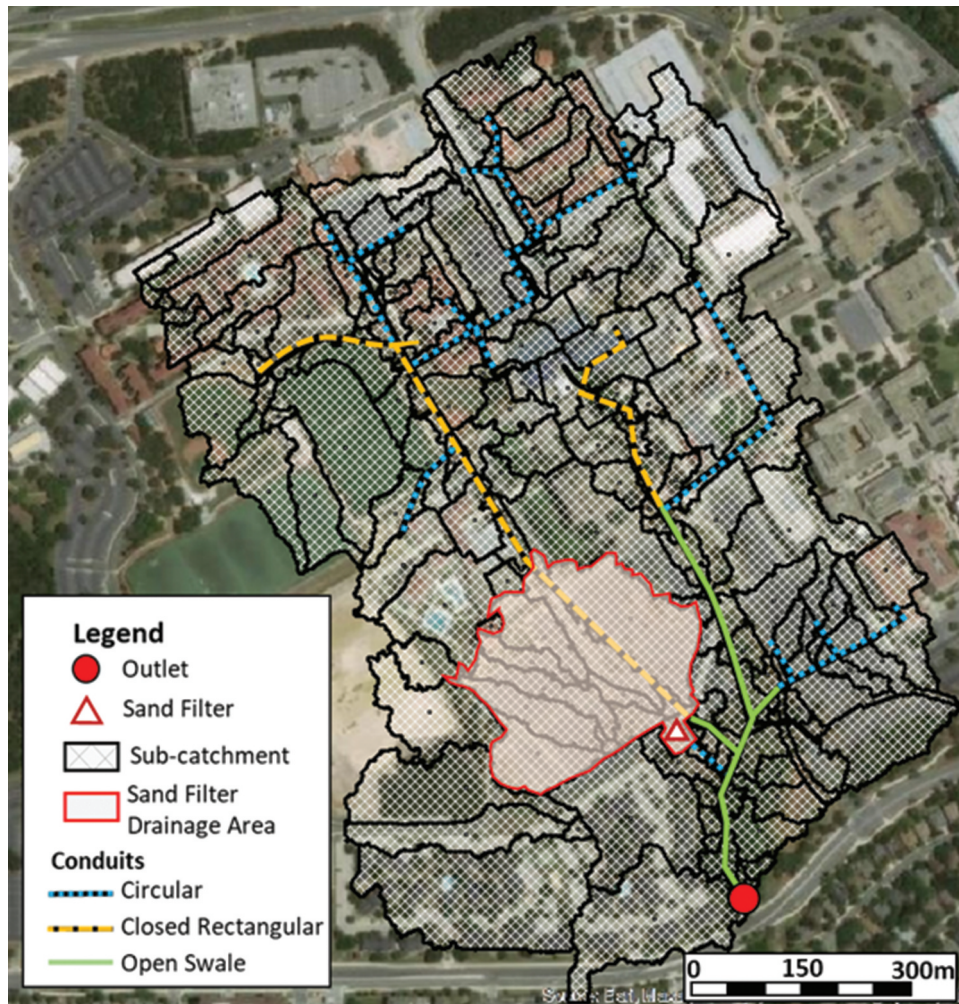


Figure 2. SWMM model of the UTSA main campus.

maximum temperatures with the Hargreaves method (Hargreaves and Samani 1982). The evaporation is significant in this study to recover the infiltration capacity of the sub-catchments during the dry days in the continuous simulation. Zarezadeh (2017) calibrated the model considering Nash-Sutcliffe efficiency (NSE), percent bias (PBIAS), and coefficient of determination (R^2). The NSE presented values of 0.84 and 0.91 for flow and depth, considered satisfactory according to Moriasi *et al.* (2007). Likewise, R^2 values were also satisfactory, with values of 0.86 and 0.77 for the same analysis. However, PBIAS presented a relatively poorer result when compared to NSE and R^2 , with values of -10 and 0.33 for flow and depth calibrations.

The land use map of the UTSA main campus was examined to identify potential locations for implementing Green Roof (GR), permeable pavement (PP) and bioretention (BR). GR was included in this study for two reasons, despite not promoting direct infiltration into the soil. First, GR is a common type of LID contributing to peak flow reduction, one of the objectives evaluated. Second, we wanted to evaluate whether GR could contribute to increasing infiltration indirectly. By reducing the peak flow, GR reduces the runoff velocity downstream, potentially increasing the proportion of runoff volume that is being infiltrated. We optimized the

combination of GR, PP, and BR as these are some of the most popular types of LIDs that are used to treat stormwater, are most commonly studied in the literature (Wang *et al.* 2017) and provide different functionality with unique contributions to the drainage system (Rodriguez *et al.* 2021). While PP and GR are responsible for treating and conveying stormwater from parking lots and roofs (in the source), BR is an end-of-pipe type of LID that treats stormwater from upstream areas. Therefore, these LIDs generally do not compete in terms of area selection.

The size of GR and PP was determined according to the maximum area of roof spaces and parking lots in each sub-catchment. It was assumed that BR would occupy a maximum of 5% of the total sub-catchment area, with a minimum of 10 m^2 of continuous pervious area, following the San Antonio River Basin LID Technical Design Guidance Manual (Dorman *et al.* 2019). The percentage of impervious area and the maximum capacity of each LID type are presented in Fig. 3. The land use analysis shows that GRs could be implemented in several sub-catchments (Fig. 3(b)), while PPs are concentrated in the north and south-central parts of the campus (Fig. 3(c)). The characteristics of each LID were selected within the recommended range (Rossman and Bernagros 2019) and are listed in Table 1.

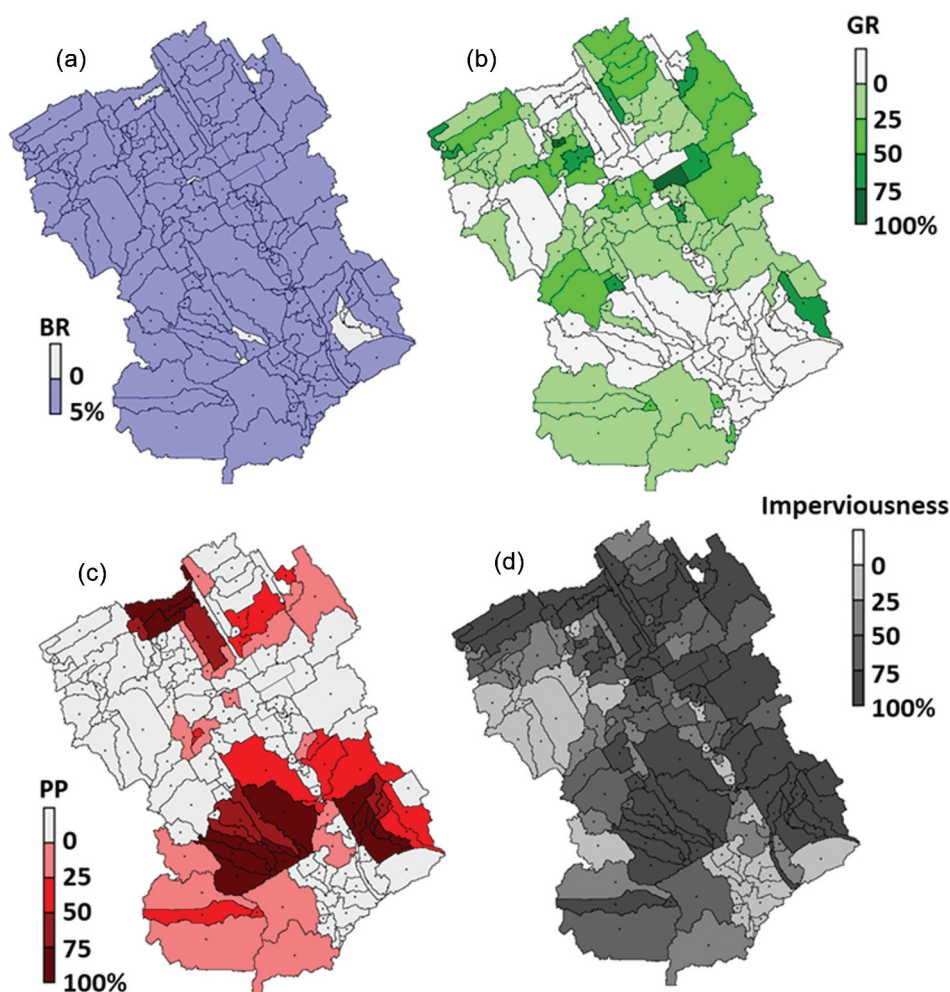


Figure 3. The maximum capacity of (a) BR, (b) GR, and (c) PP in each sub-catchment as a fraction of the area, and (d) percentage of imperviousness.

Table 1. Layer characteristics of BR, PP, and GR.

Layer	Parameter	BR	PP	GR
Surface	Berm height (mm)	0	0	0
	Vegetation volume fraction	0.15	0	0.15
	Roughness (Manning's N)	0.15	0.02	0.15
	Slope	1%	1%	30%
Soil/pavement	Thickness (mm)	500	130	120
	Void ratio	0.50	0.15	0.50
	Permeability (mm/h)	–	2500	–
	Conductivity (mm/h)	13	–	13
	Suction head (mm)	90	–	90
	Clogging factor	–	0	–
	Storage	Thickness (mm)	200	300
	Void ratio	0.75	0.75	0.50
	Seepage rate (mm/h)	13	250	–
	Clogging factor	0	0	–
	Roughness (Manning's n)	–	–	0.25

2.2 Climate change and rainfall scenarios

2.2.1 Climate models and bias correction

Rainfall projections from 32 GCMs downscaled with the Bias-Correction and Constructed Analogs version 2 (BCCAv2), and 19 with the Localized Analogs (LOCA), were obtained from the World Climate Research Programme (WCRP)'s Coupled Model Intercomparison Project Phase 5 (CMIP5) (Bureau of Reclamation 2013), totaling 51 different projections for Representative

Concentration Pathway (RCP) 4.5 and RCP 8.5. The list of all GCMs is presented in the Supplementary material (Table S1). The minimum and maximum temperatures were also acquired for each of these models to simulate evaporation, all downscaled using the same approaches.

The rainfall data were acquired from 1950 to 1999 (historical) and from 2075 to 2099 (future), since previous analysis has suggested this future period will be the driest in this century (Giacomoni *et al.* 2019). The historical data

was used to compare the models to the observed rainfall data for the same period (Station ID: GHCND.: USW00012921; Lat.: 29.54429°, Long.: -98.48395°). An additional bias correction was performed for precipitation with the daily bias correction (DBC) method (Mpelasoka and Chiew 2009). This hybrid method combines the local intensity (LOCI) (Schmidli *et al.* 2007) and daily translation (DT) (Mearns *et al.* 2009) bias corrections. Details of the bias correction applied to these projections are best described by do Lago *et al.* (2021).

2.2.2 Rainfall scenarios

A period of 25 years of historical data and the climate models for both the 1975–1999 and 2075–2099 periods were disaggregated from one-day to 15-minute resolution using the Bartlett-Lewis rectangular pulse (Rodriguez-Iturbe *et al.* 1987, 1988) with adjusting procedure method, implemented in the *HyetosMinute* R package (Kossieris *et al.* 2018). This method can be summarized in four steps: (1) the Poisson process (of rate λ) starts a storm with one cell; (2) a random number η is selected for each storm event from a gamma distribution of mean α/ν and variance α/ν^2 ; (3) secondary cells can be added to the event, with their start dictated by a Poisson process (of rate $\eta\kappa$). The duration of the event is selected from exponentially distributed average time $(1/\eta\Phi)$, after which no pulses can be added; (4) the cells are rectangular pulses with height and duration, which were randomly selected from an exponential distribution with mean $\mu\chi$ and $1/\eta$, respectively. In this study, we used the Bartlett-Lewis method with the cell intensity varying with storm duration under constant $\iota = \mu\chi/\eta$ (Kaczmarek 2014). The final storm is given by the sum of all pulses (Rodriguez-Iturbe *et al.* 1987, 1988). A total of six parameters had to be estimated: λ (d^{-1}), ϕ , ι (mm/d), κ , α , and ν (d). Ten years of observed 15-minute rainfall series (2000 to 2010) were used to calibrate the parameters considering the mean, variance, lag 1 covariance, and proportion of dry cells of the series. Although these characteristics might be nonstationary, we assumed they are constant over time and valid for future climates due to the lack of long-term rainfall series with higher temporal resolution in San Antonio. This assumption limits the full representation of future precipitation, as the temporal evolution of sub-daily characteristics is not considered. The evolutionary annealing-simplex optimization method implemented in the *HyetosMinute* package was used to estimate the parameters. A total of eleven 15-minute rainfall time series were generated: one historical (1975 to 1999) and 10 future projections (five for RCP 4.5 and five for RCP 8.5, from 2075 to 2099). The five models with the smallest error in the number of wet days and precipitation average – from the validation results of the bias-corrected precipitation – were selected to represent the future conditions. Accordingly, models with poorer performance in predicting climate characteristics were excluded to simplify the analysis.

2.3 Problem statement and optimization algorithm

In this article, the problem can be described as where in an urban watershed LID-SCMs such as BR, PP, and GR should be installed to maximize infiltration and minimize peak flow

while ensuring installation and maintenance costs are kept at a minimum. A multi-objective optimization approach is applied to address this question, generating near-optimum solutions to identify the potential tradeoffs between the objective functions described by Equations (1) to (3). Two optimization problems are proposed: (1) minimize costs and peak flow (PC), and (2) minimize costs while maximizing infiltration (IC):

$$\text{Minimize Cost} = \sum_{j=1}^M \sum_{i=1}^N p_{ij} (c_j \times A_{ij} + m_j) \quad (1)$$

$$\text{Minimize Peak Flow} = Q_p^{\text{Post LID}} \quad (2)$$

$$\text{Maximize Infiltration} = I^{\text{Post LID}} \quad (3)$$

where p_{ij} is a binary decision variable for installing a LID j at the sub-catchment i ; A_{ij} is the surface area (m^2) of the LID j at the sub-catchment i ; M is the number of LID types; N is the number of sub-catchments in a watershed; N ($\$/m^2$) includes the unit net present cost of implementation and maintenance of the LID j ; and m_j (\$) is a minimum implementation cost of LID j , which is independent of the structure size. Examples of such costs include permitting and regulatory fees, site investigations such as infiltration tests (to determine the suitability to installing the LID) and professional fees (hiring consultants, engineers or architects to assist on the design phase). In this article, we tested the implementation of three LIDs ($M = 3$): BR ($j = 1$), PP ($j = 2$), and GR ($j = 3$), with c values of \$49.9/ m^2 , \$84.7/ m^2 , and \$81.2/ m^2 for c , and m values of \$10,052, \$3,750, and \$20,824 for BR, PP and GR, respectively. These are national value guides for c and m in the US (Rossman and Bernagros 2019), but the figures can be easily updated to represent local costs. The encoding of each solution follows a similar approach to that implemented by Giacomoni and Joseph (2017) and Ogidan and Giacomoni (2016). A solution is represented by a vector chromosome with dimension $N \times M$. For each sub-catchment, one gene defines whether a particular type of LID will be installed (variable $N \times M$ in Equation 1).

SWMM is a physically-based model which can be computationally demanding, especially in models representing many sub-catchments with multiple distributed parameters (Shahrokh Hamedani *et al.* 2023). This disadvantage can be exacerbated when multiple runs (Giacomoni and Joseph 2017) and long continuous simulations are required. Because the IC required continuous simulation, we selected one representative year to optimize infiltration. Simulating the representative year, instead of the 25 years used for evaluating LID solutions, significantly reduced computation time and enabled us to perform the IC optimization. The year 1993, with annual precipitation of 818 mm (comparable to the 813 mm of average annual precipitation for the whole 1975–1999 period), was selected as the representative year. The average maximum and minimum temperatures for the 1975–1999 period were 26.8 and 14.9°C, respectively, while the values were 26.7 and 14.4°C for 1993. Matching

the minimum and maximum temperatures is also relevant for optimizing IC, as they were used to compute evaporation and could potentially affect the recovery of infiltration capacity of the sub-catchments. So, $I^{Post\ LID}$ is the total annual infiltration volume measured after LID systems have been implemented for the representative year (1993). The PC optimization was performed for the event (from the 1975–1999 period) that generated the greatest peak flow with total LID capacity on the UTSA campus, representing the worst LID performance. This event generated 115 mm of rain during seven hours on 7 October 1981. $Q_p^{Post\ LID}$ is the resultant peak flow of this event after LID placement.

The NSGA-II (Deb *et al.* 2002) was used to solve these two multi-objective problems. The NSGA-II uses three main operators during the search: (1) non-dominated sorting that classifies the solutions in fronts, (2) crowding distance to diversify the solutions and expand the search horizon, and (3) elitism to hasten the search by enabling the propagation of good solutions to new generations. The NSGA-II has been applied successfully to many water resource optimization problems, including LID placement (Giacomini and Joseph 2017, Dong *et al.* 2020), water allocation during droughts (Tsai *et al.* 2019), distribution and control of storage tanks (Fu *et al.* 2010), rehabilitation of sewer pipe networks (Yazdi *et al.* 2017, Ngamalieu-Nengoue *et al.* 2019) and location of water level sensors (Ogie *et al.* 2017) among many others. In this study, NSGA-II was implemented in Java v. 1.8.0 and the optimization was performed over 30 trials to avoid trapping in local near-optimums. These trials were run in parallel in a high-performance computer research cluster (SHAMU), an asset operated by the Research Computing Support Group of the UTSA Office of Information Technology. The optimization was performed with 100 generations and a population size of 20 individuals, with mutation and crossover rates of 0.1 and 0.9, respectively. Previous analysis showed no significant improvement in optimized results for a larger number of generations and population size but with a significant increase in computation time, extrapolating the time limit on the SHAMU Cluster.

2.4 Simulation scenarios and robustness

The RCP 4.5 and 8.5 climate change scenarios were compared with historical periods to evaluate the impacts of climate change on the hydrological cycle of the UTSA main campus. Each scenario was evaluated using 25 years of continuous simulation for historical conditions and each selected climate model for RCP 4.5 and 8.5, for the same land use. The 15-minute disaggregated rainfall series were used in the continuous simulation. The following variables were assessed in each simulated scenario: discharge peak flow and runoff, flood, and infiltration volumes. The Wilcoxon test (Wilcoxon 1992) with a significance level of 5% was performed to examine whether the hydrological conditions were statistically different under climate change scenarios compared to historical rainfall regimes. The selected solutions obtained from IC and PC were also evaluated with 25 years of continuous simulation for historical conditions and the future projected climates. The discharge peak and annual average runoff, flood, and

infiltration volumes were determined for each solution to evaluate their mitigation capacities as a function of implementation costs.

Finally, we calculated each LID solution's robustness by evaluating its performance under different rainfall scenarios. The robustness metric is based on a satisficing metric (Starr 1963) and was calculated as the fraction of scenarios under which a given infrastructure meets its design purpose. In this study, the robustness of LID solutions was calculated to evaluate their performance under different climate scenarios (Equation 4):

$$\text{Robustness} = \frac{1}{N} \sum_{p=1}^N NS_{c,j} \quad (4)$$

where N is the number of projected scenarios and $S = 1$ indicates that solution j was satisfactory and met the given goal for the projected climate c , whereas $S = 0$ indicates that solution j was not satisfactory. Classifying a solution as satisfactory or not depends on the designer's goals for the LIDs. However, the objective of LIDs placement is highly variable, and depends on multiple factors such as the characteristics of the study area and the available budget.

By definition, the main objective of LID implementation is to restore pre-development hydrological conditions. Therefore, we defined different objectives as a function of urbanization impacts on peak flow and infiltration, runoff, and flood volumes. A threshold defining the satisfactoriness of the solution was calculated with Equation (5):

$$\text{Threshold} = pHP_{pre} + (1 - p)HP_{post} \quad (5)$$

where p is a target mitigation percentage, and HP_{pre} and HP_{post} are the annual average hydrological parameter of pre- and post-development conditions, respectively, both estimated with current climate conditions (HP_{pre} defined as zero for flood volume). A solution was considered satisfactory if the resulting peak flow, runoff, and flood volumes were below a threshold. As for infiltration, the total volume should be above the threshold.

Given the subjective nature of a satisfactory infrastructure, we evaluated the robustness of the optimized solutions for multiple goals to reflect the LID's capacity to perform well under different scenarios. A sensitivity analysis of robustness as a function of p was performed, which varied from 0.1 to 1. In other words, each solution's robustness to mitigating from 10 to 100% of the urbanization impacts was calculated. These goals are transformed into threshold values (as per Equation 5) associated with infiltration, runoff, runoff volumes, and peak flow. The pre-development scenario was simulated with no impervious area and drainage infrastructure, including the sand filter basins. In addition, Manning's n of both rectangular and circular channels was set to be equal to the open swale.

3 Results and discussion

3.1 Climate models and projections

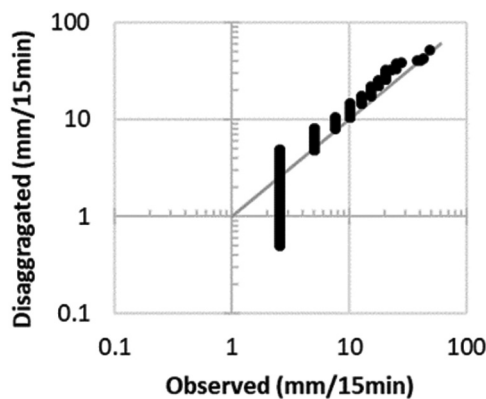
This first subsection analyzes how the climate models compare to the historical period. After the bias correction, the five selected models presented low relative errors when predicting

Table 2. Performance of selected models for daily time series from 1975 to 1999 (relative error to historical period).

Rainfall models		Averages			
		Precipitation (mm/year)	Wet period (days/year)	Min temperature (°C)	Max temperature (°C)
Historical	H	812.8	83.3	14.55	26.59
BCC-CSM (BCCAv2)	P1	803.1 (−1.1%)	80.3 (−3.6%)	14.45 (−0.7%)	26.99 (1.5%)
CESM1-BGC (BCCAv2)	P2	808.9 (−0.4%)	80.3 (−3.6%)	14.66 (0.8%)	27.13 (2.0%)
MPI-ESM-MR (BCCAv2)	P3	784.9 (−3.3%)	85.6 (2.7%)	14.72 (1.2%)	27.25 (2.5%)
BCC-CSM (LOCA)	P4	793.3 (−2.3%)	81.8 (−1.8%)	14.65 (0.7%)	26.66 (0.3%)
CanESM (LOCA)	P5	802.7 (−1.2%)	80.2 (−3.7%)	14.67 (0.8%)	26.74 (0.6%)

precipitation and temperature in San Antonio. Table 2 shows the average precipitation (mm/year), wet period (days/year), and minimum and maximum temperature (°C) for the historical and selected models for the 1975–1999 period. Despite the selected models underestimating the precipitation volume, these models could represent precipitation volumes relatively well, with errors smaller than 3.5%. The number of wet days is also represented satisfactorily, with the largest error for model P5, which underestimated the wet days by 3.7%. Minimum and maximum temperatures were overestimated when compared to the historical period. The largest relative error was 2.5% for the maximum predicted temperature with model P3.

The performance of the rainfall disaggregation method is analyzed next. The optimized parameters used in the Bartlett-Lewis rectangular pulse method, for a 15-minute temporal resolution, were 0.024 d^{-1} , 0.0051, 0.42 mm.d^{-1} , 9.96, 2.08 and 0.076 d for parameters λ , ϕ , ι , κ , α and ν , respectively. The scatter plot of observed and disaggregated rainfall cells is shown in Fig. 4. The raingauge precision for observed precipitation is 2.54 mm (0.1 in). Errors in the average precipitation depths, autocovariance, and proportion of dry periods were relatively low. It can be observed that extreme precipitation ($>10 \text{ mm}/15 \text{ min}$) was overestimated after disaggregation, which explains the greater variance error (Table 3). However, this extreme precipitation is

**Figure 4.** Scatter plot of observed and disaggregated precipitation at a time resolution of 15 minutes.**Table 3.** Statistical parameters for the observed disaggregated rainfall time series.

Parameters	Observed	Disaggregated	Error
Average (mm)	0.0219	0.0216	−1.37%
Variance (mm)	0.155	0.214	38.06%
Autocovariance Lag 1	0.0366	0.0363	−0.82%
Proportion of dry days	0.994	0.990	−0.40%

a small portion of the precipitation series (approximately 7% of the observed precipitation). The disaggregation was performed on historical and future projected series to compare those different climate scenarios. Kossieris *et al.* (2018) verified the disaggregation method used in this work over 69 years, which showed an overestimated variance for five-minute and one-hour time scales. The largest error was for the five-minute time scale, which reached approximately 50% of relative error in some months. Our results for a 15-minute temporal resolution, however, show that the disaggregated extreme values matched relatively well with the observed ones.

The climate models' projections (2075–2099) indicate that San Antonio is likely to experience a drier climate, where RCP 4.5 scenarios predict drier conditions than RCP 8.5 scenarios (Table 4). However, the standard deviation of RCP 8.5 is greater than that of RCP 4.5, which indicates a larger disagreement between projections. Zhao *et al.* (2016) evaluated the impacts of urbanization and climate change in the San Antonio River Basin using an ensemble of 17 GCMs included in the CMIP5. Their results showed that the median of the projections (RCP 4.5 and 8.5 for 2070–2099) for the monthly average precipitation is lower than the observed historical for all months, which indicates a decreasing trend in precipitation volumes. The only exceptions were February for RCP 4.5 and September for both RCPs. Table 4 shows that the infiltration volume is the most affected by climate change among total annual precipitation, evaporation, and surface runoff, with an average decrease greater than 20% compared to historical levels. Therefore, climate change projections suggest that the runoff coefficient is likely to increase. All projections presented a significantly lower infiltration, particularly for model P5 of RCP 8.5. The median of the RCP 4.5 scenario presented more similar values to the historical period, while the RCP 8.5 projections had larger disagreements (Fig. 5).

Figure 5 shows box plots including median, 1st and 3rd quartiles, minimum and maximum, and outliers for the precipitation, runoff volume, infiltration, annual peak, and flood volume for the historical, RCP 4.5, and RCP 8.5 climate projections. In the same figure, the p value calculated using the Wilcoxon test is included, where $H = 1$ rejects the null hypothesis at a significance level of 5%, meaning that the medians are significantly different. All projections for precipitation for RCP 4.5 were statistically different from (lower than) the historical, while model P5 for RCP 8.5 showed no significant difference (Fig. 5). For RCP 8.5, for instance, the P1 model had no significant difference in runoff volume compared to historical, even with lower projected precipitation volumes (Table 4). On the other hand, model P5 showed higher runoff volumes with no statistical difference in

Table 4. Historical (1975–1999) and projected (2075–2099) water balance.

	Annual average historical	Annual average and standard deviation		Difference from historical	
		RCP 4.5	RCP 8.5	RCP 4.5	RCP 8.5
Total precipitation (mm)	812.9	722.2 (±23.5)	749.4 (±68.8)	-11.1%	-7.7%
Evaporation (mm)	258.0	222.7 (±4.3)	231.3 (±6.8)	-13.7%	-10.3%
Infiltration (mm)	71.7	57.4 (±1.5)	56.7 (±3.9)	-20.0%	-21.0%
Surface runoff (mm)	483.1	442.9 (±20.3)	462.2 (±61.6)	-8.3%	-4.3%

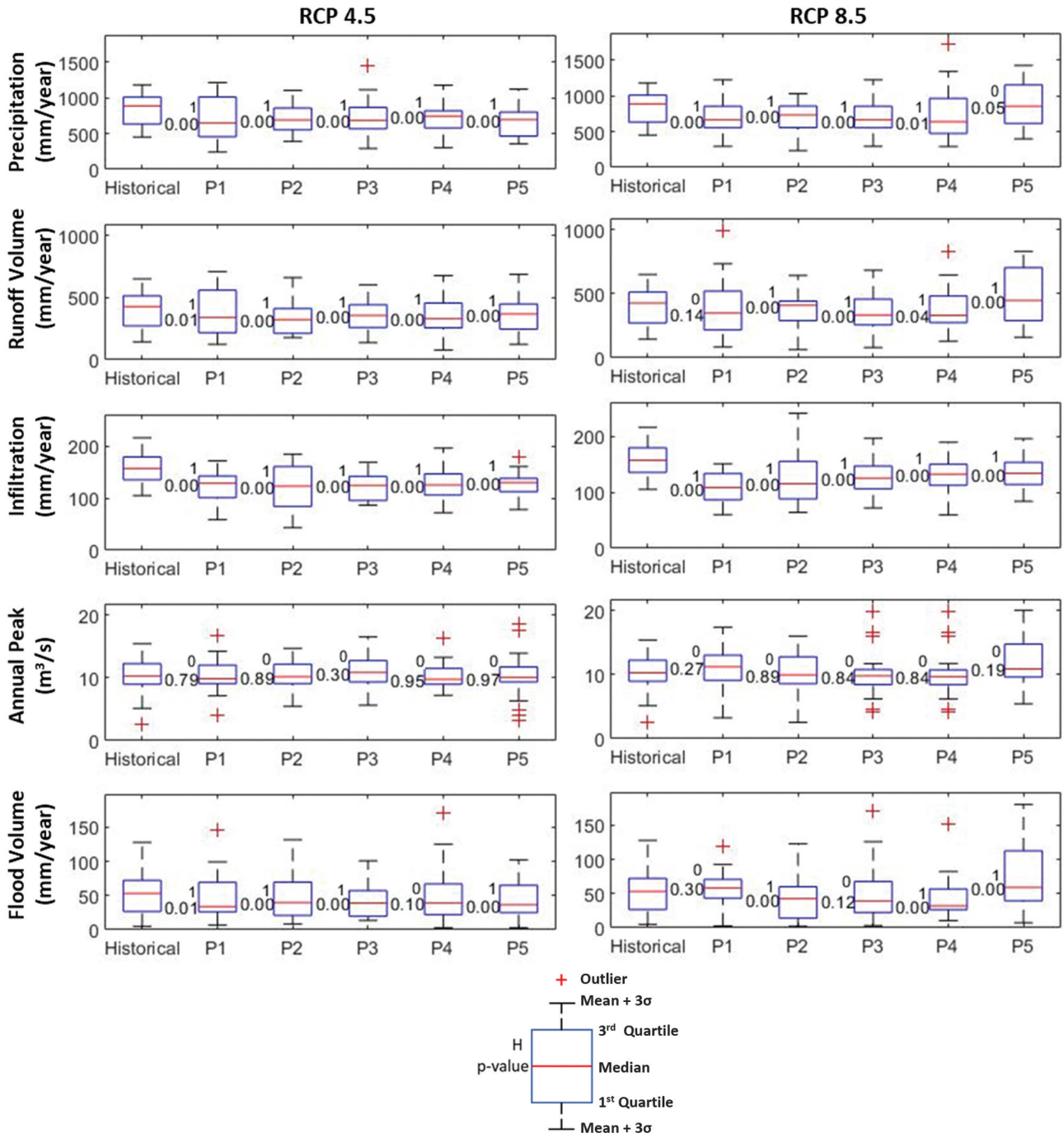


Figure 5. Climate change projections of hydrological conditions compared to historical climate, with outliers identified using standard deviation (σ). The results include p values from the Wilcoxon test. An $H = 1$ rejects the null hypothesis at a significance level of 5%.

precipitation, as the p values of the Wilcoxon test suggest. Despite no statistical difference in average annual peak flows, it can be seen that the maximum peak flows of most climate change scenarios are larger than those in the historical period.

In addition, the number of scenarios with statistically lower runoff volumes is higher than the flood volume, which means that a larger portion of runoff volume generates flooding. This finding is consistent with the study by do Lago *et al.* (2021),

which indicates that climate change is likely to intensify extreme precipitation events and magnify flood damages in San Antonio. Zhao *et al.* (2016) also found that the median annual peak flows at the San Antonio River Basin are similar to the historical conditions. However, their analysis showed large uncertainties, which pointed out the necessity of considering the maximum projected peak flows that were found to be approximately four times the median.

3.2 LID optimization

This section presents the results of the optimization scenarios. Figure 6(a) shows the non-dominated solutions for the scenarios IC and PC, where the horizontal axis shows cost (\$ million), while the primary and vertical axes show, respectively, relative infiltration change (%) and peak flow reduction (%),

respectively. Since LIDs promote infiltration and reduce peak flow, more expensive solutions with more LID units show greater infiltration increase and peak flow reduction. On the other hand, GR placement reduces the total infiltrated volume, as this type of LID is impervious and does not contribute to direct infiltration to the subsoil. Consequently, the most expensive IC solution is \$14 million with the full placement of BR and PP, whereas the most expensive PC solution is \$23 million with the full placement of all LID types.

Figure 6(b) and (c) show the numbers of LID placement for each solution on the IC and PC optimization scenarios, respectively. The results suggest that BR is a more cost-effective solution for IC, with rapid growth up to approximately 60% of its capacity at approximately \$5 million of investment. PP increased linearly and occupied a larger proportion of the watershed than BR after approximately \$10 million. GR had

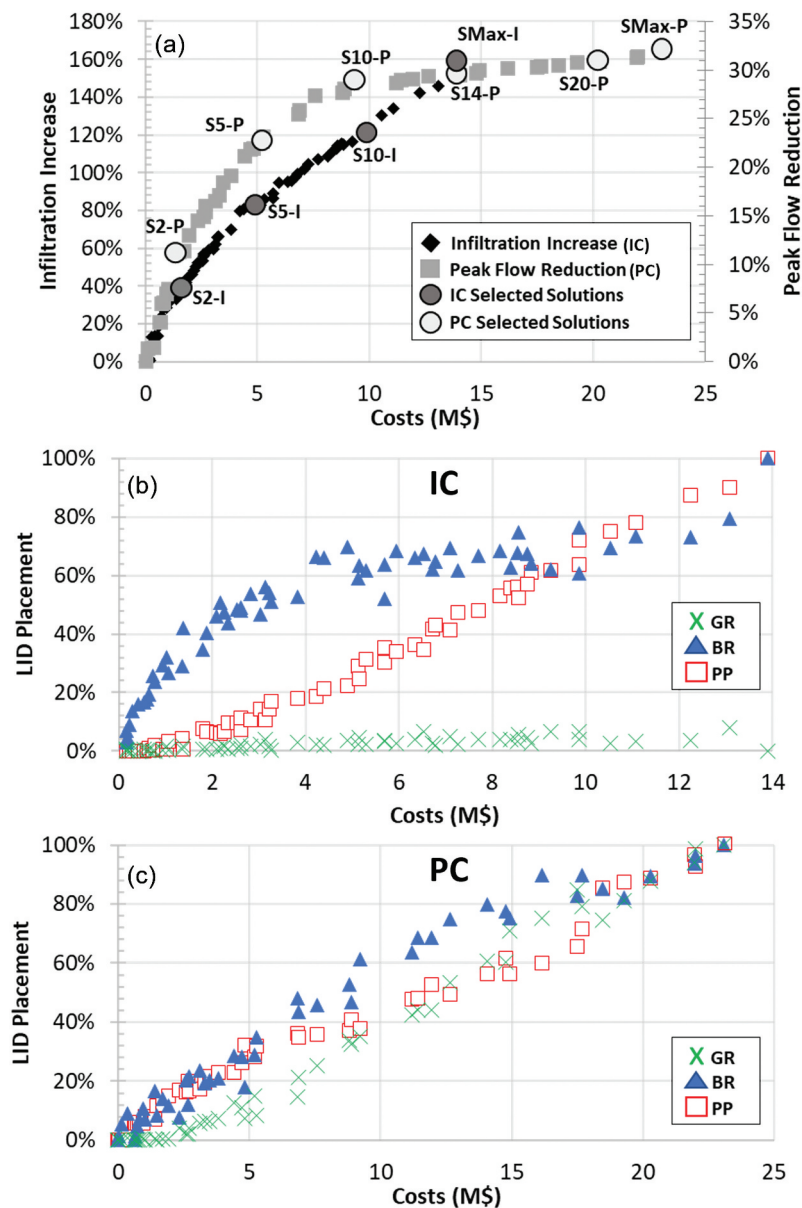


Figure 6. Non-dominated sets for IC and PC against costs (a), calculated with the representative year and peak flow (1975 to 1999), respectively. Selected solutions for further analysis are highlighted. The relative allocation of GR, BR and PP for each solution of (b) IC and (c) PC is also presented.

low application when the goal was to enhance infiltration, which shows that the stormwater retained within GR layers and later evapotranspired is larger than the potential benefits to infiltration downstream to the structure. In general, it can be seen that the benefits of adding LIDs increases more significantly when costs are relatively low. Kumar *et al.* (2022) also noted that the growth in benefits of increasing the investments is more pronounced when the overall occupation of LID is lower.

Ten solutions (four for the IC and six for the PC scenarios) were selected to enhance the analysis further. These solutions cost 2, 5, and 10 million dollars for IC (S2-I, S5-I, and S10-I), where SMax-I is the solution that resulted in maximum infiltration (full capacity of BR and PP) with a total cost of \$13.9 million (Fig. 6(a)). Smaller gaps in the costs between cheaper solutions were selected as the benefits increased more rapidly. The PC optimization showed more expensive solutions than SMax-I, as these solutions also include GR. Solutions with costs lower than \$5 million had similar percentages of PP and BR, while GR started to appear and increase with solutions of \$2.5 million or greater. BR started to prevail for the solutions between \$7 million and \$16 million, while GR increased faster than PP and reached a higher percentage within this cost range. There seems to be no preference for any LID for the most expensive solutions (greater than \$20 million). Similar solutions were selected from PC optimization results: S2-P, S5-P, S10-P, S14-P, S20-P, and SMax-P (Fig. 6), where S14-P is comparable with SMax-I with approximately the same costs. S20-P and SMax-P are not comparable with the optimized solutions of IC, since their costs are higher than the SMax-I. Figure 6 shows that the efficiency of the LID system to reduce the peak flow increases more significantly up to \$10 million, with an approximate 30% reduction of peak flow. In contrast, more expensive solutions have little effect on the peak flow reduction, such as the SMax-P (\$23 million) with an efficiency of 33%.

The GR, PP, and BR locations for the \$2 million and \$-10 million solutions optimized for infiltration and peak flow (S2-I, S10-I, S2-P, and S10-P) are illustrated in Fig. 7. It can be seen that there is a high occupation of BR for the relatively cheap solutions of IC (S2-I) with a lower number of PPs distributed over the watershed. The S2-P solution, on the other hand, presented a lower occupation of BR that was compensated with PP and GR. The expansion of LID from the S2-I to the S10-I solution was mainly through PP, while the increase in BR was less significant. The increase in PP, BR, and GR for the solutions selected from PC optimization was at the same rate, as shown in Fig. 6.

Our results indicate that LIDs should be placed preferentially near the outlet when peak flow reduction is a target objective. This pattern can be seen in the \$2 million cost solution for the peak flow optimization (S2-P), where almost no LIDs were placed in the northern area. The increase in the LID numbers for the \$10 million (S10-P) occurred closer to the outlet. Giacomoni and Joseph (2017) optimized the location of green roofs and permeable pavements. Their results also showed that placing LIDs closer to the outlet is more effective in reducing peak flows with cheaper solutions. Longer distances of flow routing cause peak attenuation and reduce

peak flows at the outlet, which explains the location preferences for the PC LID placements. On the other hand, infiltration was more independent of location; thus, LID locations for the IC-optimized solutions were more evenly distributed over the catchment. This distribution is due to the homogeneity of the soil types in this watershed. However, it can be seen that sub-catchments with a higher imperviousness (Fig. 3(d)) were selected first for BR placement. We observed that sub-catchments draining into the sand filter basin received fewer LID-SCMs for the PC problem. That was not the case for the IC problem. This difference is because the sand filter basin contributes to attenuating peak flow but does not enhance infiltration because of its impermeable liner.

In summary, our results suggest that placing BR in areas with a high imperviousness is more cost-effective when seeking improvements in infiltration. PP is then preferred when sub-catchments with high imperviousness are already treated with BR. Our findings also suggest that GR does not contribute to enhancing infiltration in areas with a relatively high temperature and number of dry days, such as San Antonio, where the climate favors losses through evaporation. Further investigations are recommended to understand better BR contributions in catchments where soil remains saturated longer. For reducing peak flows, our results show that LID can be more effective if placed near the outlet, with a less distinct preference for LID type when compared to the solutions for increasing infiltration.

3.3 Post-evaluation of optimized solutions

The 10 selected solutions (Fig. 6) were further evaluated using 25 years of continuous simulation for the historical conditions and the projected RCP 4.5 and 8.5 scenarios (Fig. 8). Figure 8 also shows the conditions for pre-development (continuous gray line) and post-developed (dashed black line). The infiltration results of each IC solution for the representative year were compared with the average of the historical 25 years (Fig. 9). These results indicate that the historical average and representative year infiltration are similar.

As expected, simulations showed better performance for peak flow and infiltration controls for the solutions optimized for PC and IC, respectively (Fig. 8). The solutions selected from IC showed better performance for runoff and flood volumes, indicating that infiltration as an objective function is more relevant to these two factors. Increasing infiltrated volumes directly reduces the runoff volume, as these are the two main components of the water balance of the system. Gao *et al.* (2021) used the technique for order preference by similarity to an ideal solution (TOPSIS) (Tzeng and Huang 2011) to optimize runoff quantity and quality with LID at a minimum cost for a maximum of 15% occupation. Their optimum solution is composed of 3.75% GR, 3.75% rain garden (a similar concept to BR), and 7.5% PP at a cost of approximately \$180 million for an area of 23.6 km² (approximately 35 times larger), with a runoff reduction of 74%. Given the proportion of the areas, their solution is comparable to this study's \$5 million solutions. S5-I has BR at approximately 60%

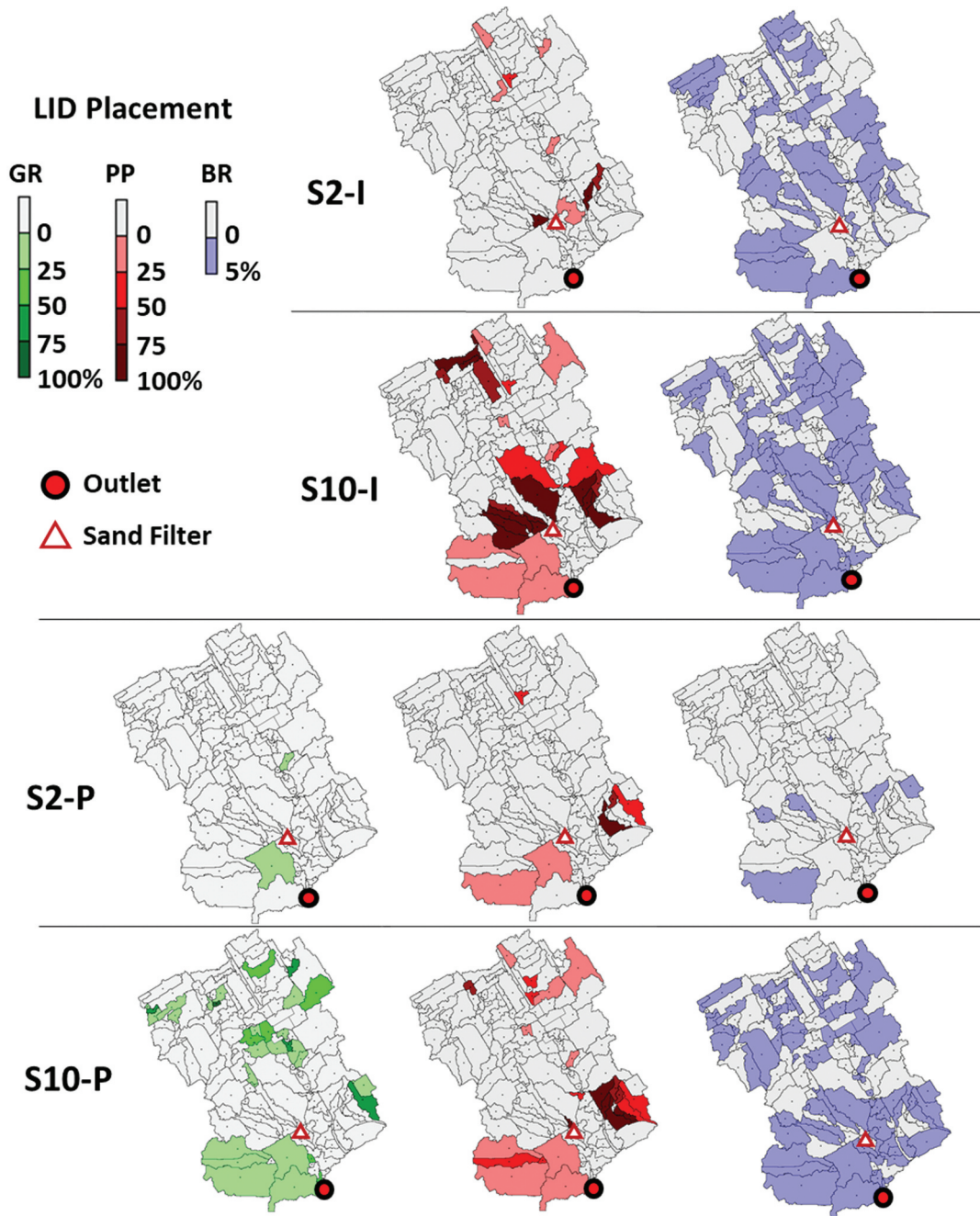


Figure 7. Cost-optimized locations of GR, PP and BR at \$2 million and \$10 million for IC and PC.

of its full capacity, PP at approximately 30%, and S5-P with approximately 25% for BR and PP, and 15% for GR.

The IC solutions presenting lower flood volumes than PC solutions is counterintuitive, as higher peak flows can surcharge the drainage system. The reason is that the IC placement of LIDs was more evenly distributed along the studied area and reduced the flood volume in a greater number of nodes. The PC optimization concentrated LIDs closer to the outlet, limiting the flood volume reduction on upstream nodes. The \$2 million solution selected from infiltration optimization (S2-I), for example, presented a slightly higher peak flow than S2-P for the historical conditions (of approximately 13 000 L/s) but with 40%

less flood volume. S2-P concentrated the LIDs on the southern portion of the campus; consequently, most of the study area achieved no benefit in hydrological conditions. S2-I, on the other hand, had placed BR in several locations across the catchment and helped reduce floods in more nodes than S2-P. The difference in flood volume between IC and PC decreases for more expensive solutions as the areas covered by LIDs with PC solutions increase. S20-P and SMax-P showed lower flood volume than any of the IC solutions, as GRs contributed to reducing runoff and alleviated the drainage system.

These results suggest that IC solutions can be more beneficial to the drainage system within the catchment where LIDs

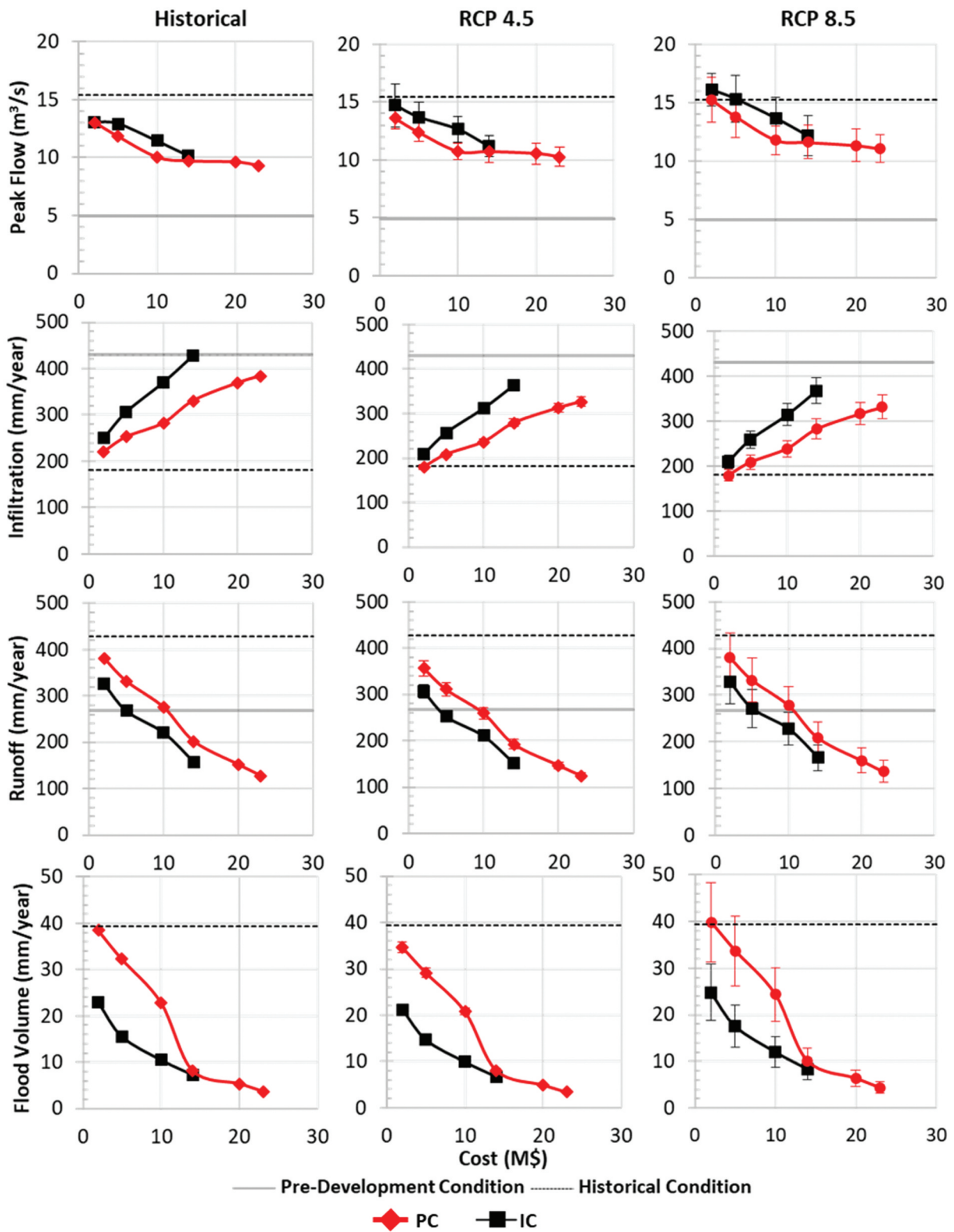


Figure 8. Performance of the selected solutions for historical conditions (left) and projected scenarios for RCP 4.5 (middle) and RCP 8.5 (right).

are installed, when compared to PC solutions with equivalent costs. However, understanding how the flood volume in nodes effectively translates into a flooded area with potential economic damages is necessary. A more precise set of solutions with the objective of minimizing local pluvial flood would

require combining the NSGA-II with two-dimensional hydrodynamic models, which is currently infeasible due to their required computational burden (do Lago *et al.* 2023). Furthermore, it is worth noting that peak flow reduction benefits are reflected downstream of the catchment. With

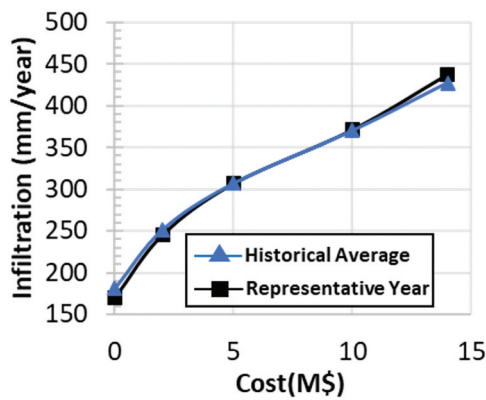


Figure 9. Annual average infiltration of 1975–1999 and total infiltration of representative year for IC solutions.

higher efficiency in reducing peak flows, the IC solutions can potentially reduce the flooding downstream. Although our results show that IC solutions have better cost–benefit ratios compared to local drainage, PC may be preferred if the goal is to minimize downstream overflows.

The selected solutions presented a similar pattern for climate change scenarios, indicating that any solution with a cost of \$2 million or higher can reestablish the historical average peak flow, infiltration, runoff, and flood volume conditions. The exceptions are S2-I, which had a higher peak flow for RCP 8.5, and S2-P, with lower infiltration volumes for RCP 4.5 and 8.5. Ghodsi *et al.* (2020) optimized the location of BR, PP, vegetated swale, and infiltrating trenches to maximize runoff reduction and minimize the cost of mitigating the impacts of climate change. Their results showed that 20% of the LID full capacity could reduce the risk of climate change-induced runoff volume by 18%. S2-I implemented 45% and 6% of the full capacity of BR and PP, respectively, whereas S2-P placed approximately 17% of BR and PP and 1% of GR.

LID implementation helps improve infiltration at the UTSA campus and can supposedly promote recharge to the Edwards Aquifer, an important water source for the city of San Antonio. This infiltration increase is consistent for all solutions and under both RCP scenarios. At \$10 million, the average infiltration is at least 300 mm, more than double the average infiltration volume for the RCP 8.5 with no LID (approximately 140 mm). The \$10 million solutions could also reduce the runoff volumes to pre-development levels. However, no solution could restore pre-development conditions of infiltration and peak flows. These results suggest that LID can help mitigate the impacts of climate change on Edwards aquifer recharge. For instance, Mooers *et al.* (2018) investigated the effects of LID on aquifer recharge in Nova Scotia, Canada. They found that LIDs increased the infiltration from 168 to 189 mm/year, while the aquifer recharge increased from 160 to 172 mm/year in a dry year. LIDs increased the infiltration and recharge in a wet year from 438 to 466 mm/year and 276 to 290 mm/year, respectively.

The simulations also showed that the increase in LID investment could reduce the uncertainties of future projected hydrological conditions, especially for RCP 8.5. This pattern is observed by shrinking the standard deviation bars considering the five selected projections, where uncertainty reduction on

flooded volume is the most noticeable (Fig. 8). The two most expensive solutions (S20-P and Smax-P) presented similar average flood volumes for the projections, with almost null standard deviations. The standard deviations for the RCP 4.5 projections are small, with similar average values, consistent with the similar median values found in Fig. 5. Climate change uncertainties can hinder water management applications due to many possibilities. Therefore, narrowing future climate conditions with LID can facilitate the development of assertive water management plans.

3.4 Robustness analysis

In this section, we evaluated the robustness of each solution based on different targets to mitigate urbanization impacts under climate change scenarios (Fig. 10). A mitigation target of 100% represents the full restoration of the pre-development hydrological conditions. This robustness analysis can facilitate decision making when facing climate change uncertainties by allowing a more thorough comparison between solutions. For instance, if the designer's objective is to promote the average infiltration to 330 mm/year (recover 60% of the infiltration lost due to urbanization), the robustness can be increased from 0 to 1 with an additional investment of \$4 million (S10-I to SMAX-I). Another example is a significant increase in robustness between the \$10 million and \$14 million solutions from peak flow optimization (S10-P and S14-P) when aiming for flood reduction. The \$10 million solution (S10-P) could only achieve a robustness of 1 for the 35 mm/year average flood volume (10% mitigation target), while the \$14 million (S14-P) presented a robustness of 1 for a flood of 15.8mm/year (60% mitigation target). These results also show how IC solutions are more robust than the PC ones for infiltration, runoff, and flood volumes. For instance, the IC optimization solution for \$10 million (S10-I) has the same robustness values as the IP solution for \$20 million when aiming to increase infiltration.

No solution was able to restore peak flow and flood volumes to pre-urbanization conditions. Runoff volume was the only hydrological parameter for which LIDs could meet the threshold for mitigating 100% of urbanization impacts due to the decrease in precipitation volumes under future climate conditions. A robustness of 1 could be achieved for SMAX-I, S20-P, and SMAX-P. In other words, these solutions would perform satisfactorily under all future climate scenarios if the analyst's objective was to reduce average runoff volumes below 268 mm/year at the UTSA campus. The robustness for peak flow presented the lowest values among the four parameters analyzed. For this hydrological parameter, 50% was the maximum mitigation target the LID solutions could achieve, and only for PC solutions with costs of \$10 million or more.

A full investment in LIDs for maximum infiltration (SMax-I) could reach pre-development infiltration with historical conditions (see Fig. 8), but no optimized solutions could restore the infiltration to pre-urbanization levels for future climate. The reduction in projected precipitation volume for future climate scenarios resulted in zero robustness for all IC and PC solutions. This outcome shows the importance of considering climate change when planning LID placement. Although the infrastructure might perform

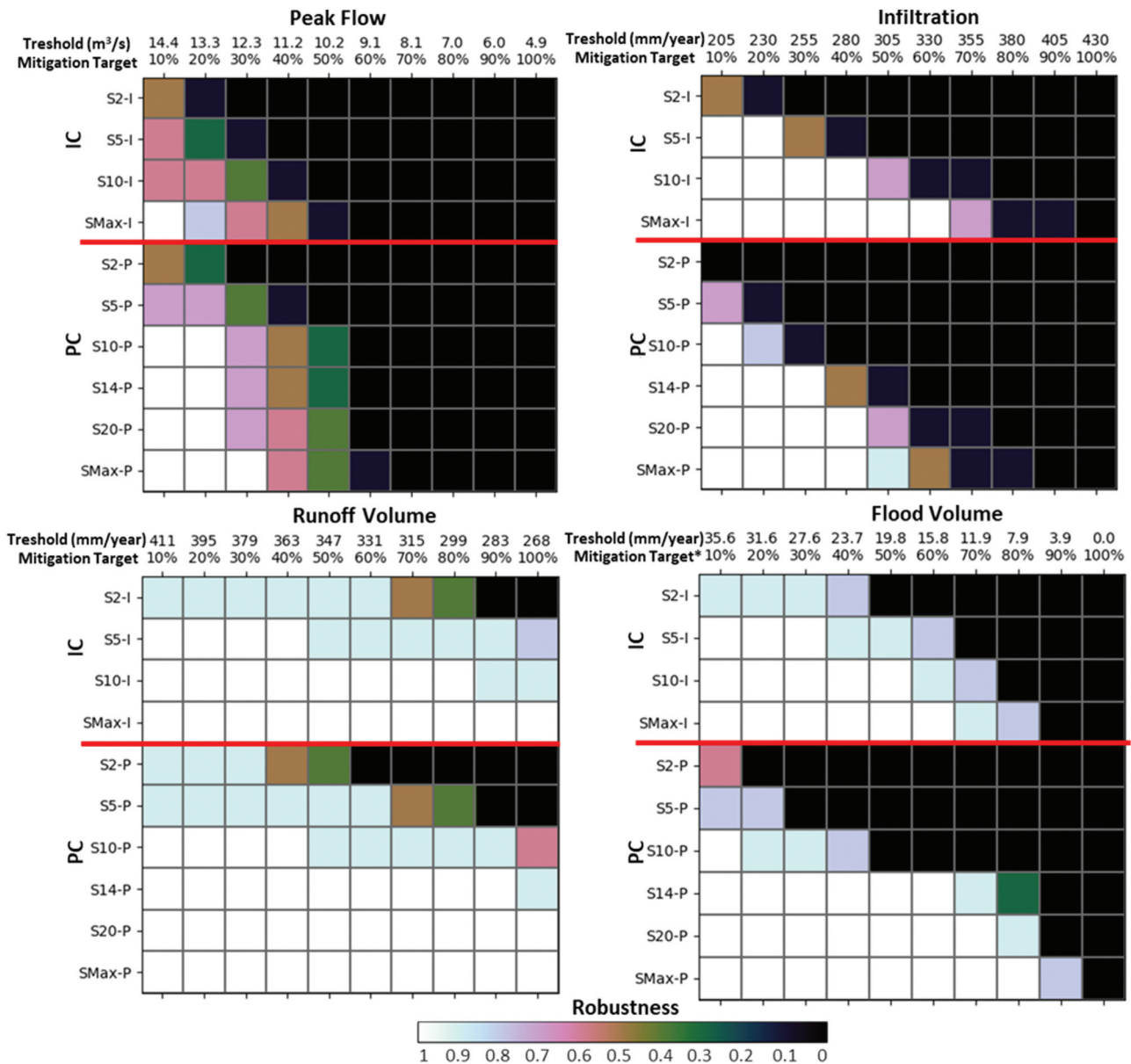


Figure 10. Robustness of optimized solutions. Lighter colors represent higher robustness. Note:* Mitigation target is based on no flood volume.

as expected for the historical conditions used for the design, it can fail under future conditions.

4 Summary and conclusions

This study applied a simulation-optimization framework to optimize the location and type of LIDs in a small urban catchment and evaluate the performance of the solutions to mitigate climate change. The approach includes (1) treating the climate data with bias correction and rainfall disaggregation, (2) optimization by combining SWMM with NSGA-II, and (3) evaluating the solutions according to their hydrological performance and robustness. Our methods addressed the difficulties regarding optimization when a continuous simulation is required, which can be replicated in other catchments. This approach allowed us to maximize infiltration while minimizing costs (IC), which was lacking in the literature. For comparison, we have also optimized peak flow

against cost (PC), a common objective used to optimize LID placements. The solutions were analyzed according to their hydrological performance and robustness under different climate projections.

Our findings indicate that BR in highly impervious sub-catchments are preferred to enhance the cost-benefit ratio when aiming for increasing infiltration, followed by PP. On the other hand, LIDs placed near the outlet result in a better cost-benefit ratio when the goal is to decrease peak flows, with a lower distinction between LID types when compared to IC solutions. IC optimization solutions proved to be more effective in increasing infiltration and reducing flood volumes within the catchment. The IC optimization distributed the LID cells more evenly across the catchment when compared to the PC, which reduces runoff loads in a larger portion of the local drainage system. In contrast, PC solutions were more efficient in reducing peak flow at the outlet, with a better potential to mitigate floods in the downstream area.

Our results showed that IC solutions effectively enhanced infiltration and could contribute to mitigating climate change impacts in catchments with a projected drier climate. However, the robustness of IC and PC solutions showed how climate change could compromise the expected performance of LID infrastructure. For instance, the most expensive IC solution increased the infiltration volume to pre-development conditions, which could not be achieved in future climate scenarios due to lower precipitation volumes. Our findings highlight the necessity of accounting for climate change during LID design.

The optimization solutions show that LIDs improve infiltration rates, potentially benefiting aquifer recharge. However, the proposed methodology does not account for aquifer recharge since not all infiltrated volume directly translates into groundwater recharge. In future studies, we recommend applying a groundwater model to assess the LID benefits of the solutions for recharge volumes and how they can contribute to reducing the impacts of climate change. Furthermore, our study lacks an investigation of stormwater quality improvements by LIDs. The future drier climates can increase pollutant loads during dry deposition periods, increasing the concentration of washed-off pollutants during storms and degrading stormwater quality. Therefore, future studies should also investigate how LID practices could improve the quality of infiltrated water and, consequently, the quality of groundwater reaching the aquifers. Finally, our investigations did not include flood analysis downstream of the studied area. We recommend investigating LID effects on downstream floods to evaluate the benefits of peak flow reduction. Although the IC solutions improved infiltration, flood volumes, and runoff volume within the catchment area, PC solutions on peak flow can benefit downstream more. We also suggest further investigating optimizing LID placement to enhance infiltration under different climates. The studied catchment is under a relatively dry and hot climate, where evapotranspiration is significant. Although GR negatively affected infiltration in this study, this type of LID structure could be beneficial to increase infiltrated volumes in catchments where stormwater losses due to evapotranspiration are lower. Finally, we suggest investigating how updates in climate models, such as changes from CMIP5 to CMIP6, affect optimized LID solutions' projected performance.

Disclosure statement

No potential conflict of interest was reported by the authors.

Funding

The study received financial support from the Transportation Consortium of South-Central States (Tran-SET) - University Transportation Center for Region 6 Project under grant #18HSTSA02. Additionally, funding was provided by the Coordination for the Improvement of Higher Education Personnel (Capes), under the Proex program. EMM thanks Univ Montpellier I-SITE Excellence Program & Campus France [Grant 139529Q/3281199].

ORCID

Eduardo Mário Mendiondo  <http://orcid.org/0000-0003-2319-2773>

References

- Ahmed, K., Shahid, S., and Nawaz, N., 2018. Impacts of climate variability and change on seasonal drought characteristics of Pakistan. *Atmospheric Research*, 214, 364–374. doi:10.1016/j.atmosres.2018.08.020
- Aich, V., et al., 2016. Flood projections within the Niger River Basin under future land use and climate change. *Science of the Total Environment*, 562, 666–677. doi:10.1016/j.scitotenv.2016.04.021
- Ayanlade, A., et al., 2018. Rainfall variability and drought characteristics in two agro-climatic zones: an assessment of climate change challenges in Africa. *Science of the Total Environment*, 630, 728–737. doi:10.1016/j.scitotenv.2018.02.196
- Azari, B. and Tabesh, M., 2022. Urban storm water drainage system optimization using a sustainability index and LID/BMPs. *Sustainable Cities and Society*, 76, 103500. doi:10.1016/j.scs.2021.103500
- Baek, S.S., et al., 2015. Optimizing low impact development (LID) for stormwater runoff treatment in urban area, Korea: experimental and modeling approach. *Water Research*, 86, 122–131. doi:10.1016/j.watres.2015.08.038
- Batalini de Macedo, M., et al., 2022. Low impact development practices in the context of United Nations Sustainable Development Goals: a new concept, lessons learned and challenges. *Critical Reviews in Environmental Science and Technology*, 52 (14), 2538–2581. doi:10.1080/10643389.2021.1886889
- Berne, A., et al., 2004. Temporal and spatial resolution of rainfall measurements required for urban hydrology. *Journal of Hydrology*, 299 (3–4), 166–179. doi:10.1016/S0022-1694(04)00363-4
- Brown, R.A. and Hunt, W.F., 2012. Improving bioretention/biofiltration performance with restorative maintenance. *Water Science and Technology*, 65 (2), 361–367. doi:10.2166/wst.2012.860
- Carolus, J.F., et al., 2020. Nutrient mitigation under the impact of climate and land-use changes: a hydro-economic approach to participatory catchment management. *Journal of Environmental Management*, 271, 110976. doi:10.1016/j.jenvman.2020.110976
- Charlesworth, S.M., 2010. A review of the adaptation and mitigation of global climate change using sustainable drainage in cities. *Journal of Water and Climate Change*, 1 (3), 165–180. doi:10.2166/wcc.2010.035
- Clavet-Gaumont, J., et al., 2017. Probable maximum flood in a changing climate: an overview for Canadian basins. *Journal of Hydrology: Regional Studies*, 13, 11–25.
- Cronshey, R., 1986. *Urban hydrology for small watersheds* (No. 55). US Department of Agriculture, Soil Conservation Service, Engineering Division.
- Deb, K., et al., 2002. A fast and elitist multiobjective genetic algorithm: NSGA-II. *IEEE Transactions on Evolutionary Computation*, 6 (2), 182–197. doi:10.1109/4235.996017
- de Macedo, M.B., et al., 2017. Learning from the operation, pathology and maintenance of a bioretention system to optimize urban drainage practices. *Journal of Environmental Management*, 204, 454–466. doi:10.1016/j.jenvman.2017.08.023
- de Macedo, M.B., et al., 2021. Low impact development practices in the context of United Nations Sustainable Development Goals: a new concept, lessons learned and challenges. *Critical Reviews in Environmental Science and Technology*, 1–44.
- do Lago, C.A., et al., 2023. Generalizing rapid flood predictions to unseen urban catchments with conditional generative adversarial networks. *Journal of Hydrology*, 618, 129276. doi:10.1016/j.jhydrol.2023.129276
- do Lago, C.A.F., et al., 2021. Assessing the impact of climate change on transportation infrastructure using the hydrologic-footprint-residence metric. *Journal of Hydrologic Engineering*, 26 (5), 04021014. doi:10.1061/(ASCE)HE.1943-5584.0002076
- Dong, F., et al., 2020. Towards efficient low impact development: a multi-scale simulation-optimization approach for nutrient removal at the urban watershed. *Journal of Cleaner Production*, 269, 122295. doi:10.1016/j.jclepro.2020.122295
- Dorman, T., et al., 2019. *San Antonio River Basin low impact development technical design guidance manual*. v1 (Issue May). San Antonio River Authority.
- Eckart, K., McPhee, Z., and Bolisetti, T., 2018. Multiobjective optimization of low impact development stormwater controls. *Journal of Hydrology*, 562, 564–576. doi:10.1016/j.jhydrol.2018.04.068

- Fletcher, T.D., Andrieu, H., and Hamel, P., 2013. Understanding, management and modelling of urban hydrology and its consequences for receiving waters: a state of the art. *Advances in Water Resources*, 51, 261–279. doi:10.1016/j.advwatres.2012.09.001
- Fu, G., Khu, S.-T., and Butler, D., 2010. Optimal distribution and control of storage tank to mitigate the impact of new developments on receiving water quality. *Journal of Environmental Engineering*, 136 (3), 335–342. doi:10.1061/(ASCE)EE.1943-7870.0000161
- Gao, C., et al., 2020. Effects of climate change on peak runoff and flood levels in Qu River Basin, East China. *Journal of Hydro-Environment Research*, 28, 34–47. doi:10.1016/j.jher.2018.02.005
- Gao, J., et al., 2021. A distribution optimization method of typical LID facilities for Sponge city construction. *Ecology & Hydrobiology*, 21 (1), 13–22.
- Ghodsii, S.H., et al., 2020. Optimal design of low impact development practices in response to climate change. *Journal of Hydrology*, 580, 124266. doi:10.1016/j.jhydrol.2019.124266
- Giacomoni, M.H. and Joseph, J., 2017. Multi-objective evolutionary optimization and Monte Carlo simulation for placement of low impact development in the catchment scale. *Journal of Water Resources Planning and Management*, 143 (9), 04017053. doi:10.1061/(ASCE)WR.1943-5452.0000812
- Giacomoni, M., Olivera, F., and Do Lago, C., 2019. *Assessing the impacts of super storm flooding in the transportation infrastructure—case study: San Antonio, Texas*. Available from: https://repository.lsu.edu/transect_pubs/42.
- Giacomoni, M.H., Zechman, E.M., and Brumbelow, K., 2012. Hydrologic footprint residence: environmentally friendly criteria for best management practices. *Journal of Hydrologic Engineering*, 17 (1), 99–108. doi:10.1061/(ASCE)HE.1943-5584.0000407.
- Giese, E., et al., 2019. Assessing watershed-scale stormwater green infrastructure response to climate change in Clarksburg Maryland. *Journal of Water Resources Planning and Management*, 145 (10), 05019015.
- Hargreaves, G.H. and Samani, Z.A., 1982. Estimating potential evapotranspiration. *Journal of the Irrigation & Drainage Division*, 108 (3), 225–230.
- Heinemann, A.B., et al., 2017. Climate change determined drought stress profiles in rainfed common bean production systems in Brazil. *Agricultural and Forest Meteorology*, 246, 64–77. doi:10.1016/j.agrfor.2017.06.005
- Helmi, N.R., et al., 2019. Developing a modeling tool to allocate low impact development practices in a cost-optimized method. *Journal of Hydrology*, 573, 98–108. doi:10.1016/j.jhydrol.2019.03.017
- Herman, J.D., Reed, P.M., Zeff, H.B. and Characklis, G.W., 2015. How should robustness be defined for water systems planning under change? *Journal of Water Resources Planning and Management*, 141 (10), 04015012.
- Huang, C.L., et al., 2018. Optimization of low impact development layout designs for megacity flood mitigation. *Journal of Hydrology*, 564, 542–558. doi:10.1016/j.jhydrol.2018.07.044
- Kaczmarek, J., Isham, V., and Onof, C., 2014. Point process models for fine-resolution rainfall. *Hydrological Sciences Journal*, 59 (11), 1972–1991.
- Kasprzyk, J.R., et al., 2013. Many objective robust decision making for complex environmental systems undergoing change. *Environmental Modelling & Software*, 42, 55–71.
- Kossieris, P., et al., 2018. A rainfall disaggregation scheme for sub-hourly time scales: coupling a Bartlett-Lewis based model with adjusting procedures. *Journal of Hydrology*, 556, 980–992. doi:10.1016/j.jhydrol.2016.07.015
- Kumar, S., et al., 2022. Multi-objective optimization for stormwater management by green-roofs and infiltration trenches to reduce urban flooding in central Delhi. *Journal of Hydrology*, 606, 127455.
- Kundzewicz, Z.W., et al., 2018. Uncertainty in climate change impacts on water resources. *Environmental Science & Policy*, 79, 1–8.
- Liu, Y., et al., 2017. Optimal implementation of green infrastructure practices to minimize influences of land use change and climate change on hydrology and water quality: case study in spy run creek watershed, Indiana. *Science of the Total Environment*, 601, 1400–1411.
- Marcos-Garcia, P., Lopez-Nicolas, A., and Pulido-Velazquez, M., 2017. Combined use of relative drought indices to analyze climate change impact on meteorological and hydrological droughts in a Mediterranean basin. *Journal of Hydrology*, 554, 292–305. doi:10.1016/j.jhydrol.2017.09.028
- McPhail, C., et al., 2018. Robustness metrics: how are they calculated, when should they be used and why do they give different results? *Earth's Future*, 6 (2), 169–191.
- Mearns, L.O., et al., 2009. A regional climate change assessment program for North America. *Eos, Transactions American Geophysical Union*, 90 (36), 311. doi:10.1029/2009EO360002
- Mooers, E.W., et al., 2018. Low-impact development effects on aquifer recharge using coupled surface and groundwater models. *Journal of Hydrologic Engineering*, 23 (9), 04018040. doi:10.1061/(ASCE)HE.1943-5584.0001682
- Moriasi, D.N., et al., 2007. Model evaluation guidelines for systematic quantification of accuracy in watershed simulations. *Transactions of the ASABE*, 50 (3), 885–900. doi:10.13031/2013.23153
- Mpelasoka, F.S. and Chiew, F.H.S., 2009. Influence of rainfall scenario construction methods on runoff projections. *Journal of Hydrometeorology*, 10 (5), 1168–1183. doi:10.1175/2009JHM1045.1
- Nam, W.-H., et al., 2015. Drought hazard assessment in the context of climate change for South Korea. *Agricultural Water Management*, 160, 106–117. doi:10.1016/j.agwat.2015.06.029
- Ng, J.Y., Fazlollahi, S., and Galelli, S., 2020. Do design storms yield robust drainage systems? How rainfall duration, intensity, and profile can affect drainage performance. *Journal of Water Resources Planning and Management*, 146 (3), 04020003.
- Ngamalieu-Nengoue, U.A., Iglesias-Rey, P.L., and Martínez-Solano, F.J., 2019. Urban drainage networks rehabilitation using multi-objective model and search space reduction methodology. *Infrastructures*, 4 (2), 35. doi:10.3390/infrastructures4020035
- Ogidan, O. and Giacomoni, M., 2016. Multiobjective genetic optimization approach to identify pipe segment replacements and inline storages to reduce sanitary sewer overflows. *Water Resources Management*, 1–16. doi:10.1007/s11269-016-1373-z
- Ogie, R.I., et al., 2017. Optimal placement of water-level sensors to facilitate data-driven management of hydrological infrastructure assets in coastal mega-cities of developing nations. *Sustainable Cities and Society*, 35, 385–395. doi:10.1016/j.scs.2017.08.019
- Peel, M.C., Finlayson, B.L., and McMahon, T.A., 2007. Updated world map of the Köppen-Geiger climate classification. *Hydrology and Earth System Sciences*, 11 (5), 1633–1644. doi:10.5194/hess-11-1633-2007
- Reclamation, B.O., 2013. *Downscaled CMIP3 and CMIP5 climate and hydrology projections: release of downscaled CMIP5 Climate Projections, Comparison with preceding Information, and Summary of User Needs*. US Department of the Interior, Bureau of Reclamation, 47.
- Refsgaard, J.C., et al., 2013. The role of uncertainty in climate change adaptation strategies—A Danish water management example. *Mitigation and Adaptation Strategies for Global Change*, 18 (3), 337–359. doi:10.1007/s11027-012-9366-6
- Rodriguez, M., et al., 2021. Exploring the spatial impact of green infrastructure on urban drainage resilience. *Water*, 13(3), 1789.
- Rodriguez-Iturbe, I., Cox, D.R., and Isham, V., 1987. Some models for rainfall based on stochastic point processes. *Proceedings of the Royal Society of London. A. Mathematical and Physical Sciences*, 410 (1839), 269–288.
- Rodriguez-Iturbe, I., Cox, D.R., and Isham, V., 1988. A point process model for rainfall: further developments. *Proceedings of the Royal Society of London. A. Mathematical and Physical Sciences*, 417 (1853), 283–298.
- Rossmann, L.A. and Bernagros, J.T., 2019. *National stormwater calculator user's guide—Version 2.0. 0.1*. Office of Research and Development, US Environmental Protection Agency.
- Schmidli, J., et al., 2007. Statistical and dynamical downscaling of precipitation: an evaluation and comparison of scenarios for the European Alps. *Journal of Geophysical Research: Atmospheres*, 112 (D4). doi:10.1029/2005JD007026
- Shahrokh Hamedani, A., Do Lago, C., and Giacomoni, M.H., 2023. Exploring near-optimal locations for bioretention systems in catchment scale using many-objective evolutionary optimization. *Urban Water Journal*, 20 (7), 813–830. doi:10.1080/1573062X.2023.2211557
- Shrestha, S., Bach, T.V., and Pandey, V.P., 2016. Climate change impacts on groundwater resources in Mekong Delta under representative

- concentration pathways (RCPs) scenarios. *Environmental Science & Policy*, 61, 1–13. doi:10.1016/j.envsci.2016.03.010
- Sim, I., et al., 2018, April. Analysis of effect of temporal resolution in projected future rainfall data on estimating future rainfall intensity-duration-frequency curves. In *EGU General Assembly Conference Abstracts*, 2139.
- Starr, M.K., 1963. *Product design and decision theory*. Prentice-Hall series in engineering design. Studies in engineering design. Prentice-Hall: Hoboken NJ. Available from: <https://cir.nii.ac.jp/crid/1130000796213587968> [Accessed September 2021].
- Sun, S., et al., 2017. Urban hydrologic trend analysis based on rainfall and runoff data analysis and conceptual model calibration. *Hydrological Processes*, 31 (6), 1349–1359. doi:10.1002/hyp.11109
- Sun, Y., Tong, S., and Yang, Y.J., 2016. Modeling the cost-effectiveness of stormwater best management practices in an urban watershed in Las Vegas Valley. *Applied Geography*, 76, 49–61. doi:10.1016/j.apgeog.2016.09.005
- Taghizadeh, S., Khani, S., and Rajaei, T., 2021. Hybrid SWMM and particle swarm optimization model for urban runoff water quality control by using green infrastructures (LID-BMPs). *Urban Forestry & Urban Greening*, 60, 127032.
- Tansar, H., Duan, H.F., and Mark, O., 2022. Catchment-scale and local-scale based evaluation of LID effectiveness on urban drainage system performance. *Water Resources Management*, 36 (2), 507–526. doi:10.1007/s11269-021-03036-6.
- TNRIS, Texas Natural Resources Information System, 2020. *Strategic mapping program (StratMap)*. Bexar County Lidar [online]. Available from: <https://tnris.org/stratmap/elevation-lidar/> [Accessed July, 2020].
- Tsai, W.-P., et al., 2019. Drought mitigation under urbanization through an intelligent water allocation system. *Agricultural Water Management*, 213, 87–96. doi:10.1016/j.agwat.2018.10.007
- Tzeng, G.-H. and Huang, J.-J., 2011. *Multiple attribute decision making: methods and applications*. CRC press: New York.
- Wang, M., et al., 2017. A framework to support decision making in the selection of sustainable drainage system design alternatives. *Journal of Environmental Management*, 201, 145–152.
- Wang, Q., et al., 2020. Individual and combined impacts of future land-use and climate conditions on extreme hydrological events in a representative basin of the Yangtze River Delta, China. *Atmospheric Research*, 236, 104805.
- Wang, Z., et al., 2018. Climate change enhances the severity and variability of drought in the Pearl River Basin in South China in the 21st century. *Agricultural and Forest Meteorology*, 249, 149–162. doi:10.1016/j.agrformet.2017.12.077
- Wilcoxon, F., 1992. Individual comparisons by ranking methods. In: *Breakthroughs in statistics: Methodology and distribution*. New York, NY: Springer, 196–202.
- Yazdi, J., et al., 2017. Application of multi-objective evolutionary algorithms for the rehabilitation of storm sewer pipe networks. *Journal of Flood Risk Management*, 10 (3), 326–338. doi:10.1111/jfr3.12143
- Yin, J., et al., 2018. A copula-based analysis of projected climate changes to bivariate flood quantiles. *Journal of Hydrology*, 566, 23–42. doi:10.1016/j.jhydrol.2018.08.053
- Yoon, J.H., et al., 2018. Concurrent increases in wet and dry extremes projected in Texas and combined effects on groundwater. *Environmental Research Letters*, 13 (5), 054002.
- Yu, Y., et al., 2022. New framework for assessing urban stormwater management measures in the context of climate change. *Science of the Total Environment*, 813, 151901.
- Zarezaeh, V., 2017. *coupling hydrologic and urbanization modeling: a multi-scale investigation to enhance urban water resource systems sustainability*. The University of Texas at San Antonio.
- Zhang, S., and Pan, B., 2014. An urban storm-inundation simulation method based on GIS. *Journal of Hydrology*, 517, 260–268.
- Zhao, G., Gao, H., and Cuo, L., 2016. Effects of urbanization and climate change on peak flows over the San Antonio River Basin, Texas. *Journal of Hydrometeorology*, 17 (9), 2371–2389. doi:10.1175/JHM-D-15-0216.1